

Robust C-PdNi-CNF Sandwich-Structured Catalyst for Suzuki Reactions and Experimental Study on the Mechanism

Yu Su, Ying Li, Chunping Li, Tong Xu, Yinghui Sun,* and Jie Bai*

Cite This: *ACS Omega* 2022, 7, 29747–29754

Read Online

ACCESS |



Metrics & More

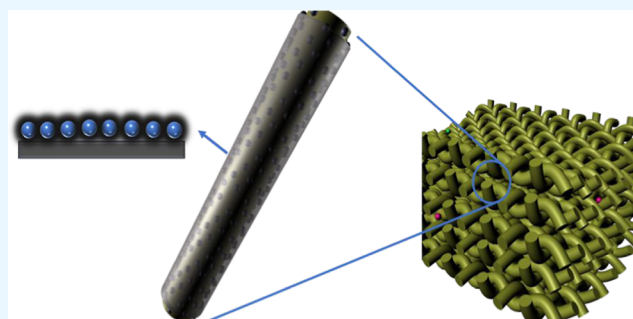


Article Recommendations



Supporting Information

ABSTRACT: The stability of metal nanoparticles is one of the key issues for their catalytic applications. In this study, we fabricated a sandwich structure to protect the metal nanoparticles. A carbon layer was used to wrap the PdNi nanoparticles on the carbon fiber, and the whole preparation process was simple and green. Electron transfer occurs between the carbon layer and the metal nanoparticles, making the two more closely combined. As a catalyst for the Suzuki reaction, it exhibits highly efficient catalysis and excellent stability. The calculated TOF reaches 18 662 h⁻¹. After nine cycles, there was almost no decrease in performance. Additionally, we found that the addition of iodobenzene into the chlorobenzene reaction system could significantly improve the chlorobenzene conversion, and we proved that the catalyst has fine activity and stability with a bright future in commercial applications. The possible catalytic mechanism of Suzuki reaction was proposed based on experimental results. This study provides a simple and green method to prepare encapsulated metal nanoparticle catalysts and gives a deep insight into Suzuki reaction.



fine activity and stability with a bright future in commercial applications. The possible catalytic mechanism of Suzuki reaction was proposed based on experimental results. This study provides a simple and green method to prepare encapsulated metal nanoparticle catalysts and gives a deep insight into Suzuki reaction.

INTRODUCTION

Heterogeneous catalysts based on noble metal nanoparticles have attracted widespread attention due to their high catalytic efficiency in many liquid phase catalytic reactions. Due to the excellent catalytic performance of palladium nanoparticles (Pd NPs) in C–C coupling reaction,^{1,2} pollutant degradation, hydrogenation,³ and C–H activation,⁴ palladium-based heterogeneous catalysts have been extensively studied by researchers.

The catalytic performance of Pd NPs mainly depends on their chemical environment. The electron distribution on the surface of the nanoparticles could be adjusted by the coordination of nanoparticles, and the catalyst exhibits excellent activity in the specified reaction.⁵ For example, the strong interaction between the metal and support not only stabilizes the metal particles but also tailors the electronic state of metal by using a hydroxyapatite supporter.⁶ Heteroatom doping is another method for fixing metal particles and regulating their surface charge.⁷ Generally, the small size of Pd NP could obtain a large accessible surface area and reveal high catalytic activity. However, with the decreasing size of Pd NPs, the surface energy increase, which makes the nanoparticles easier to agglomerate, and the performance of the nanoparticles is reduced or loses its activity. Therefore, the stability of Pd NP is also a key issue for its further application.^{8,9} One solution is to use supports, such as carbon,¹⁰ Al₂O₃,^{11,12} mesoporous silica,^{13,14} and carbon nanofibers,¹⁵ to immobilize nanoparticles. The large surface area of supports and strong interaction between Pd NPs and the support could ensure the

full dispersion of nanoparticles and prevent aggregation. The specific diameter of the carrier pores can also prevent the continuous growth of nanoparticles. Another solution is to wrap the nanoparticles with layered materials. The coating layer could restrict the mobility of nanoparticles from corroding and agglomeration during the reaction. For example, the encapsulated transition metal nanoparticles into carbon nanotubes can effectively prevent 3d transition metal from corroding in acidic media. Meanwhile, electron transfer between the carbon layer and metal makes the catalyst exhibits high stability and activity in oxygen reduction and hydrogen evolution reaction.^{16,17}

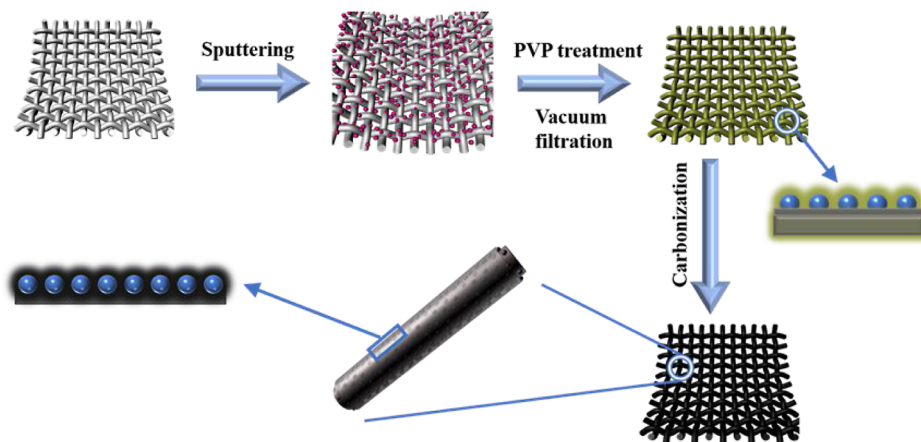
Suzuki reaction is a typical Pd NP catalytic reaction,¹⁸ which plays an important role in the synthesis of pharmaceutical intermediates¹⁹ and fine chemicals.²⁰ Our previous study has reported that the addition of Ni atoms into the Pd NPs catalyst could improve the activity in the Suzuki reaction due to the synergy between Pd and Ni.¹⁵ Meanwhile, the replacement of noble metal Pd by non-noble metal Ni without activity loss is an efficient way to decrease the cost of catalyst. Herein, we proposed a simple and new method to encapsulate Pd–Ni

Received: April 17, 2022

Accepted: August 3, 2022

Published: August 15, 2022



Scheme 1. Schematic Diagram of x -C-PdNi-CNFs Preparation

nanoparticles in a sandwich structure.^{21,22} The nanoparticles are protected by the carbon layer to achieve multiply multiple high-efficiency utilization of the catalyst in the Suzuki reaction. Besides, we found that when iodobenzene and chlorobenzene coexist in the reaction system, the conversion of chlorobenzene was improved remarkably. Thus, a possible reaction mechanism was proposed.

EXPERIMENTAL SECTION

The support was prepared by electrospinning. The spinning solution was obtained by dissolving 0.5 g polyacrylonitrile (PAN) and 0.1 g beta-cyclodextrin (β -CD) in 4.5 g dimethylformamide. When PAN and β -CD were completely dissolved, the homogeneous precursor solution was electrospun onto aluminum foil at a distance of 18 cm and a voltage of 16 kV to obtain a CD-PAN film.

The Pd and Ni metals were loaded on the CD-PAN film by the sputtering method. A spark ablation nanoparticle generator was used to synthesize PdNi NP with a voltage of 1 kV and a current of 5 mA.²³ In this process, a pair of cylindrical PdNi electrodes were placed in the holder. Then, the carrier gas (N_2) passed through the gap between the electrodes at a flow rate of 5 L/min. The metal nanoparticles were generated from the ablation of the PdNi electrode, which was condensed and deposited on the CD-PAN nanofiber membrane to obtain PdNi/CD-PAN.

To prepare the sandwich structure catalysts, the PVP solution was poured on the PdNi/CD-PAN membrane, and then, the sample was filtered using a vacuum pump. After drying the surface, the film was further dried at 100 °C for 1 h. Finally, it was calcined in a tube furnace in a N_2 atmosphere at 250 °C for 2 h and then at 400 °C for 2 h at a rate of 2 °C/min. After the samples were cooled down to room temperature, x -C-PdNi@CNFs samples were obtained ($x = 1, 3, 6,$ and 9 , corresponding to the concentration of PVP solution = 1, 3, 6, and 9%, respectively). For comparison, we also prepared a sample without the addition of PVP and labeled it C-CNFs. The preparation was similar to the step of x -C-PdNi@CNFs but without adding the PVP.

The procedure of testing the catalytic performance of x -C-PdNi@CNFs in the Suzuki coupling reaction was similar to our precious work.²⁴ In a typical run, aryl halide or its derivatives (0.5 mmol), phenylboronic acid (0.55 mmol), base (0.5 mmol), and catalyst were mixed into the C_2H_5OH/H_2O ($v/v = 4/3$) solution at 80 °C. After reaction for 1 h, the used

catalyst was collected and washed thoroughly with a mixture of ethanol and water. Then the dried catalyst was reused for the next cycle. The conversion and product selectivity were analyzed by GC.

RESULTS AND DISCUSSION

Morphology and Physicochemical Properties of x -C-PdNi-CNFs. Scheme 1 illustrates the preparation process of

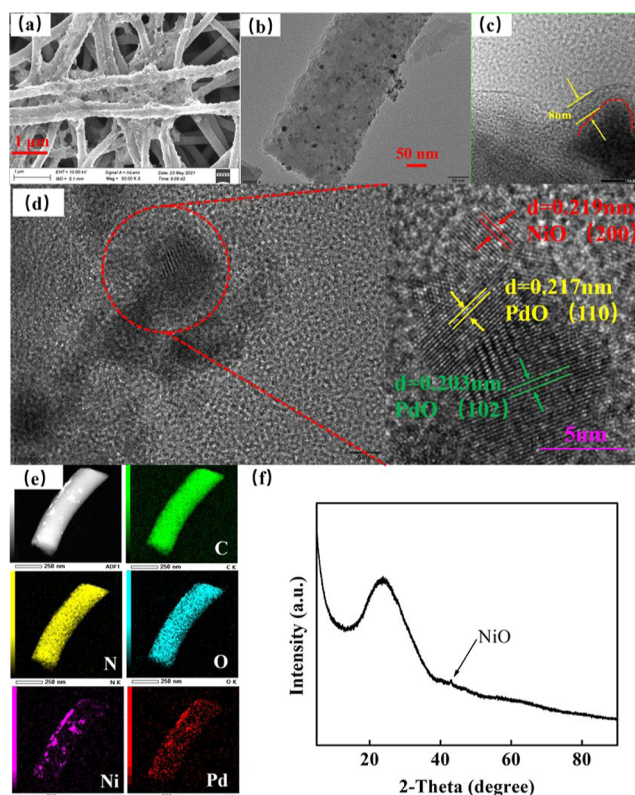


Figure 1. Surface morphologies of 3-C-PdNi-CNFs, (a–d) are its SEM, TEM, and HRTEM images. (e) EDX maps of C, N, O, Ni, and Pd. (f) XRD patterns of 3-C-PdNi-CNFs.

the x -C-PdNi@CNFs. First, a β -CD doped PAN fiber membrane was prepared by electrospinning method, and then, the PdNi nanoparticles were loaded on the fiber membrane by an electric spark sputtering method. After

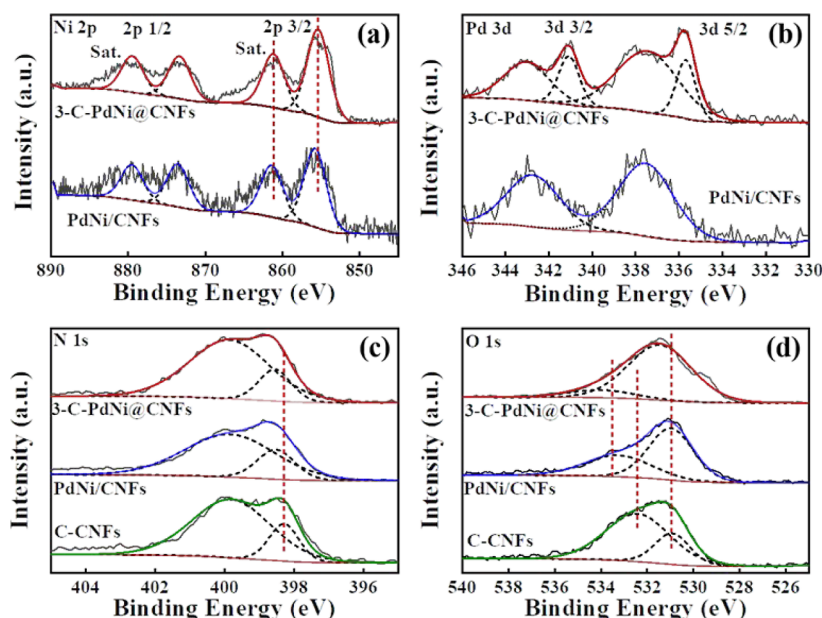


Figure 2. (a) Ni 2p (b) Pd 3d XPS spectra of 3-PdNi-CNFs and PdNi/CNFs (c) N 1s (d) O 1s XPS spectra of 3-PdNi-CNFs, PdNi/CNFs, and C-CNFs.

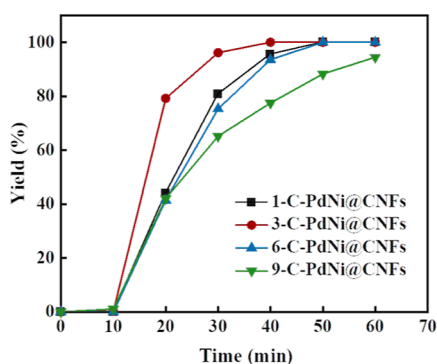


Figure 3. Time course of the biphenyl yield by *x*-C-PdNi-CNFs. Reaction conditions: aryl halides or their derivatives (0.5 mmol), phenylboronic acid or the various derivatives of it (0.55 mmol), K_2CO_3 (0.5 mmol), and catalyst (1 mg) were added into the solvent mixture. Air atmosphere, 80 °C, and without any stirring during the reaction.

treating the PdNi-loaded fiber membrane with PVP solution and filtering using a vacuum pump, the sample was carbonized in a N_2 atmosphere at 400 °C. The morphology of the prepared catalyst was tested by scanning electron microscopy (SEM) and transmission electron microscopy (TEM). As shown in Figures S1–S4, the introduction of β -CD and the sputtering of nanoparticles did not change the structure of the PAN fiber membrane. However, PVP treatment results in an increase of the fiber diameter from 300 to 370 nm and the formation of cross-linking between the fibers.

After treating the sample at a high temperature in a N_2 atmosphere, the desired catalyst is obtained. As shown in Figures 1a,b and S5–S7, the fiber diameter is reduced by about 20 nm due to the decomposition and carbonization of PVP. It is supported by the Fourier transform infrared (FTIR) spectra, shown in Figure S8. The vibrations of the functional groups of PVP disappear in *x*-C-PdNi@CNFs, indicating that the PVP in PVP-CD-PAN is completely converted into a carbon layer. The TEM image in Figure 1c shows that a carbon layer of about 8 nm is wrapped on the carbon fiber substrate, while the

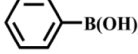
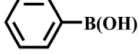
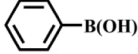
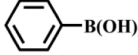
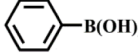
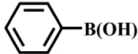
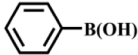
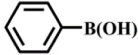
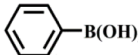
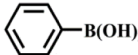
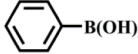
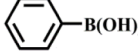
high-resolution TEM (HRTEM) analysis (Figure 1d) confirmed that the NiO and PdO particles are also protected in the carbon layer. The carbon protective film can ensure the effective catalytic reaction of the nanoparticles, and can also realize the multiple uses of a large number of nanoparticles. The element mapping images (Figure 1e) show the even distribution of Pd and Ni species supported on CNFs.

The composition and structural properties of samples are explored by a combination of ICP, X-ray diffraction (XRD), and Brunauer–Emmett–Teller. In 3-C-PdNi@CNFs, the contents of Pd and Ni elements are 0.43 and 0.99 wt %, respectively. The N_2 adsorption–desorption isotherms reveal that the surface area of CD-CNFs is $29 \text{ m}^2 \text{ g}^{-1}$, while the specific surface area of 3-C-PdNi@CNFs increases to $128 \text{ m}^2 \text{ g}^{-1}$. The increase in the surface area resulted from the coating of the carbon layer. From XRD patterns (Figure 1f), the prepared sample exhibit the diffraction of 23.8° , suggesting the formation of graphite carbon species after carbonization.

The small peak at $2\theta = 43.275^\circ$ is attributed to the (111) crystal plane of NiO (JCPDS 47-1049). Note that the XRD diffraction peak of nickel oxide is shifted to a small angle by 0.175° compared to the standard PDF card of NiO (JCPDS 47-1049), suggesting that the unit cell volume of NiO is slightly increased. It might be caused by the insertion of palladium into the crystal lattice of NiO. Moreover, owing to the low content of Pd in the catalyst, the palladium species is not observed in the XRD pattern.

XPS analysis was performed to obtain the surface electronic properties of the samples. The overall XPS spectra of the samples (Figure S9) show that 3-C-PdNi@CNFs and PdNi@CNFs contain C, O, N, Ni, and Pd elements, while C-CNFs contain C, O, and N elements. The Ni 3d XPS spectra (Figure 2a) show two doublet peaks. The two peaks at 873.4 and 855.4 eV are attributed to Ni $2p_{1/2}$ and $2p_{3/2}$ of Ni^{2+} species, respectively.^{25,26} The other two peaks at 879.4 and 861.2 eV are the shake-up satellite peaks of Ni^{2+} . By comparing 3-C-PdNi-CNFs and PdNi/CNFs, it is found that the binding energy of Ni in 3-C-PdNi-CNFs shifts to the low binding

Table 1. 3-C-PdNi-CNF-Catalyzed Suzuki Reaction between Aryl Halides and Arylboronic Acid^a

Entry	Aryl halide	Arylboronic acid	Conversion (%)	Selectivity (%)
1			99	99
2			93	99
3			90	98
4			91	99
5			99	99
6			99	99
7			99	99
8			99	99
9			99	99
10			99	99
11			96	99
12			—	—

^aReaction conditions: aryl halides (0.5 mmol), phenylboronic acid or the various derivatives of it (0.55 mmol), K₂CO₃ (0.5 mmol), and catalyst (5 mg) were added into the solvent mixture. Air atmosphere, 80 °C, and without any stirring during the reaction.

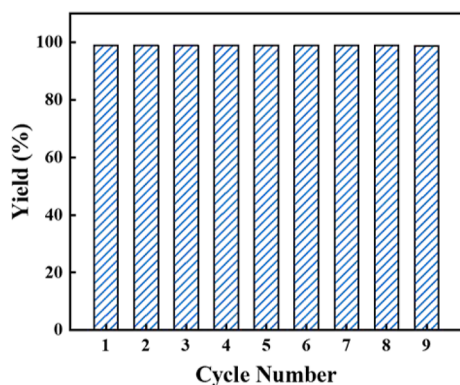


Figure 4. Reusability of the 3-C-PdNi-CNF catalyst.

energy, indicating that electron transfer from carrier to metal. At present, it is believed that the oxidative addition step of the first step of the Suzuki reaction is an electrophilic reaction, so the electrons obtained by Pd are beneficial to participate in the first step reaction. The Pd 3d XPS spectrum of PdNi/CNFs

only shows two peaks at 337.2 and 341.2 eV, which are attributed to Pd(II).^{27,28}

A similar fitting analysis for the Pd 3d XPS spectrum of 3-C-PdNi@CNFs (Figure 2b) suggests that two additional peaks appear on it besides Pd²⁺ peaks owing to the ex both Pd⁰ and Pd²⁺.²⁹ It suggests that the carbon layer reduces Pd²⁺ to Pd⁰. Because the carbon layer protects the metal nanoparticles, palladium can exist in the form of metal. The N 1s peaks (Figure 2c) at 398.5 and 399.8 eV are attributed to pyridine-like and pyrrole-like nitrogen, respectively.³⁰ The O 1s XPS spectra (Figure 2d) are fitted with peaks at 531.0 and 533.3, which are assigned to surface oxygen vacancies and chemisorbed oxygen, respectively.³¹ Note that the peaks of two O species and pyrrole-like N species shift to the higher binding energy side. Considering the changes in surface electronic properties of Pd and Ni, we conclude that the electron transfer occurred between the coating layer and metal nanoparticles. This is due to the existence of electron transfer between the carrier and the metal, which facilitates the binding between the carrier and the PdNi, which improves the catalytic performance of the Pd. As a result, the palladium–nickel nano-

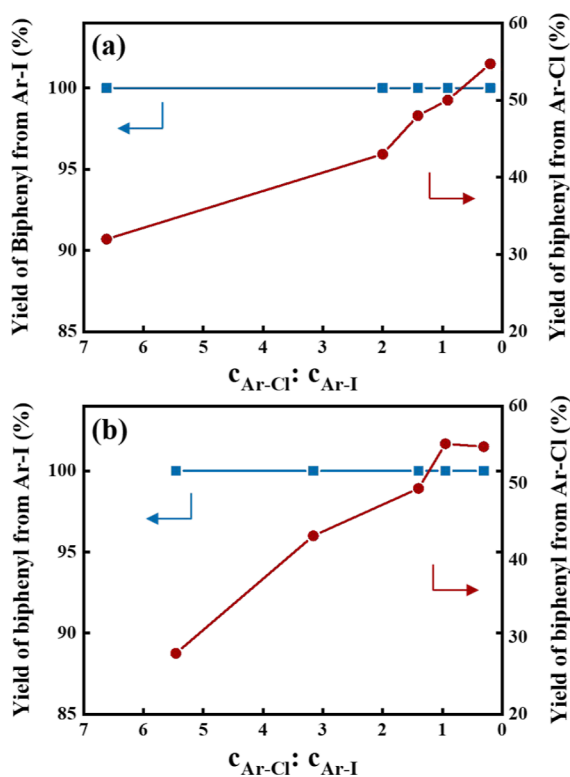


Figure 5. Result of the reaction when iodobenzene and chlorobenzene coexist. Catalyst (a) is 3-C-PdNi@CNFs, and catalyst (b) is a commercial Pd/C catalyst. The blue curve indicates that the biphenyl is derived from iodobenzene, and the red curve indicates that the biphenyl is derived from chlorobenzene.

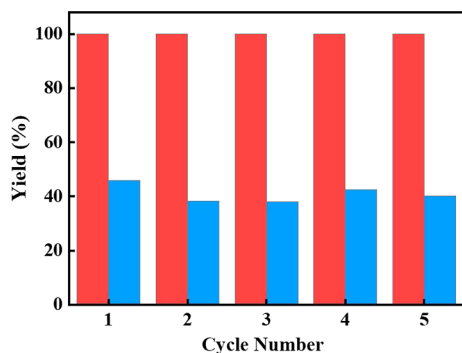


Figure 6. Recycling of the 3-C-PdNi@CNF-catalyzed Suzuki reaction with the coexistence of Ar-I and Ar-Cl derivatives. Orange bars indicate that the biphenyl is derived from iodobenzene, and yellow bars indicate that the biphenyl is derived from chlorobenzene.

particles can be more firmly attached to the carrier, which provides the possibility for multiple uses and efficient use of the catalyst.

Application of *x*-C-PdNi@CNFs in Suzuki Coupling between Iodobenzene and Phenylboronic Acid. The catalytic performance of the *x*-C-PdNi@CNFs was evaluated for the Suzuki coupling reaction, which is a typical Pd-nanoparticle-catalyzed reaction. First of all, we explored the influence of the PVP concentration used in sample preparation on the activity of the Suzuki coupling reaction. As shown in Figure 3, the sample prepared with a PVP concentration of 3% (3-C-PdNi@CNF) exhibits the fastest reaction rate in the Suzuki reaction between aryl iodobenzene (Ar-I) and

arylboronic acid (Ar-B(OH)₂). Moreover, the linear relationship between $\ln(C_0/C_t)$ and reaction time suggests (Figure S10) that the Suzuki coupling over *x*-C-PdNi@CNF samples is a first-order reaction for iodobenzene, which is consistent with the previous result obtained based on Pd/CeO₂-RE catalyst.³¹ Meanwhile, it is also concluded that the concentration of PVP does not affect the order of the reaction.

Taking the activity into consideration, the 3-C-PdNi@CNF catalyst is chosen for further exploration of catalytic generality. The results of the Suzuki coupling reaction with different aryl iodobenzene and arylboronic acid are summarized in Table 1. It can be found that by using the 3-C-PdNi@CNF catalyst, the aryl iodobenzene (Table 1, entry 1) is effectively converted into the corresponding coupling product with yields of 98%. It suggests that the designed 3-C-PdNi@CNF catalyst shows excellent activity for the Suzuki reactions. The calculated TOF is 18 662 h⁻¹, which is much higher than most palladium catalysts (Table S1). When the aryl iodide induced by the -CH₃, -OCH₃, or -NO₂ group is used as a substrate, the yield of corresponding coupling products is still higher than 88% (Table 1, entry 2–10).

The reusability of the catalyst was tested by using iodobenzene and phenylboronic acid as probe reactants of the Suzuki reaction. As shown in Figure 4, the yield of the product can maintain >98% even after being recycled 9 times. For comparison, we also performed the recycling experiment for the reaction over PdNi/CNFs, the performance of the catalyst declined to lower than 90% after 5 cycles (Figure S11), confirming that the carbon layer is able to protect the nanoparticles during the reaction.

Application of 3-C-PdNi@CNFs in Suzuki Coupling between Halogenated Benzene and Phenylboronic Acid. The activity of Suzuki coupling between halogenated benzene and phenylboronic acid is listed in Table 1, entries 1, 11, and 12. The conversion of Ar-I and Ar-Br is 99 and 96%, respectively, while the selectivity to corresponding coupling products of two reactions is equal with a value of 99%, suggesting that conversion of iodobenzene is easier than bromobenzene in the Suzuki reaction. However, chlorobenzene can not be converted by the 3-C-PdNi@CNF catalyst. For the Suzuki coupling reaction, it is generally accepted that the oxidative addition step of halobenzene and palladium is the rate-limiting step.³² Because the reaction with chlorobenzene requires high activation energy, chlorobenzene is unreactive under the optimized condition (Table 1 entry 12) for the Suzuki coupling reaction.

Interestingly, our experimental results show that when chlorobenzene and iodobenzene co-exist in the reaction system, the chlorobenzene can also participate in the reaction with high conversion of chlorobenzene. The conversion of chlorobenzene gradually increases with increasing the ratio of iodobenzene to chlorobenzene in the system (Figure 5a). When the ratio of iodobenzene to chlorobenzene is 4:1, the yield is reached (55%). That is to say, the yield of Suzuki coupling between chlorobenzene and arylboronic acid is increased from 0 to 55% with the addition of iodobenzene. We also explored the universality of the promotion effect of iodobenzene based on commercial palladium-carbon catalyst. As shown in Figure 5b, a similar result was obtained, suggesting that the discovery can be extended to commercial Pd/C catalysts. Moreover, we also tested the recycling ability of catalysts in this reaction system. As shown in Figure 6, the

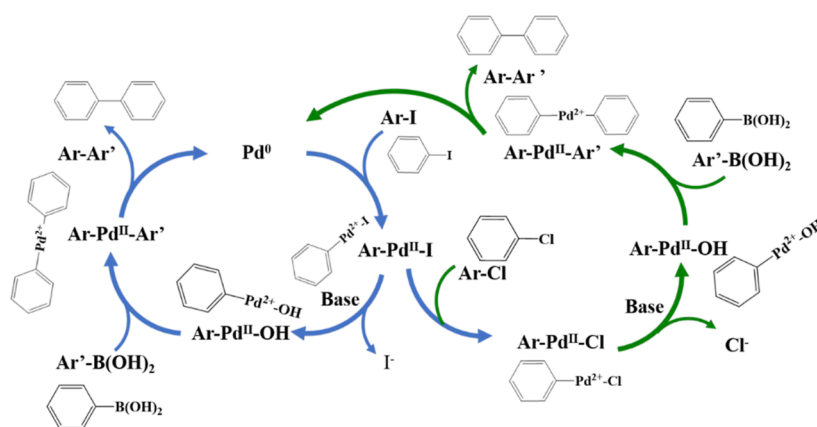


Figure 7. Mechanism of the Suzuki coupling reaction with the coexistence of Ar-I and Ar-Cl.

Table 2. 3-C-PdNi-CNF-Catalyzed Suzuki Reaction with the Coexistence of Ar-I and Ar-Cl Derivates^a

entry	aryl halide	X-aryl halide	phenylboronic acid	biphenyl yield (%)	x-biphenyl yield (%)
1	I-Ar	Cl-Ar-NO ₂	Ar-B(OH) ₂	99	31.8
2	I-Ar	Cl-Ar-CN	Ar-B(OH) ₂	99	26.7
3	I-Ar	Cl-Ar-CH ₃	Ar-B(OH) ₂	99	
4	I-Ar	Cl-Ar-OCH ₃	Ar-B(OH) ₂	99	
5	I-Ar	Cl-Ar	Ar-B(OH) ₂	99	35.3
6	I-Ar	I-Ar			

^aReaction conditions: the ratio of iodobenzene to X-aryl halide is 1.5:1.

chlorobenzene conversion over 3-C-PdNi@CNFs can maintain >38% even after being recycled for the fifth time.

To further illustrate the reason for the high chlorobenzene conversion when chlorobenzene and iodobenzene co-exist in the reaction system, a possible reaction mechanism is proposed based on the abovementioned analysis and published work^{32,33} (Figure 7). The reaction is initiated by the oxidative addition step, that is, Ar-X interacts with Pd⁰ to generate Ar-Pd²⁺-X species, which has been proved to be the rate-determining step. In our case, Ar-I, rather than Ar-Cl, attacks the palladium nanoparticles, forming an Ar-Pd²⁺-I intermediate. Then, a part of the Ar-Pd²⁺-I reacts with Ar-Cl to generate Ar-Pd²⁺-Cl. Thus, the high activation energy of the reaction between Ar-Cl and Pd⁰ to form Ar-Pd²⁺-Cl is replaced by an easier reaction (Ar-I reacts with Pd⁰) followed by the halogen-exchange reaction, leading to the reduction of the overall activation barrier. Finally, both Ar-Pd²⁺-I and Ar-Pd²⁺-Cl react with OH⁻ and Ar-B(OH)₂ to produce Ar-Pd²⁺-Ar. The Ar-Ar product is generated through the reductive elimination of Ar-Pd²⁺-Ar.

Based on the above-speculated reaction mechanism, we believe that the intermediate Ar-Pd²⁺-X is more prone to nucleophilic reactions than Pd⁰ alone. Table 2 entry 1 and 2 shows that chlorobenzene with electron-withdrawing groups can participate in the reaction, and the yield of pure chlorobenzene is consistent. Meanwhile, as shown in Table 2 entries 3 and 4, it is difficult for chlorobenzene with electronic donating groups to take part in the reaction, and the corresponding substituted biphenyls are obtained. All these observations further confirm the speculation. Besides, we excluded the interference of the Ullmann reaction on the yield of biphenyl (Table 2 entry 6).

CONCLUSIONS

In this work, a sandwich structured x-C-PdNi@CNF catalyst, consisting of carbon film coating, encapsulated Pd-Ni nanoparticles, and carbon support, was synthesized by a simple, green, and environmentally friendly method. The prepared 3-C-PdNi@CNF catalyst exhibited excellent catalytic performance and ultra-high cycle stability in the Suzuki coupling reaction. The calculated TOF reaches 18 662 h⁻¹. After 9 cycles, there is almost no decrease in performance. Our experimental study innovatively proved that the addition of iodobenzene into the chlorobenzene reaction system could facilitate the reaction between chlorobenzene and phenylboronic acid. When the ratio of iodobenzene to chlorobenzene is 4:1, the yield is reached (55%). We extended this discovery to Pd/C catalysts, and the same phenomenon occurred. This discovery has positive significance for large-scale synthesis. Meanwhile, the possible mechanism for the Suzuki coupling reaction with the coexistence of chlorobenzene and iodobenzene in the reaction system was proposed.

ASSOCIATED CONTENT

Supporting Information

The Supporting Information is available free of charge at <https://pubs.acs.org/doi/10.1021/acsomega.2c02400>.

Additional data of characterization of catalysts (SEM, TEM, FTIR, and XPS data), Arrhenius plots of Suzuki reaction, reusability of the PdNi/CNFs, catalytic activity evaluation, and product mass spectrometry data (PDF)

AUTHOR INFORMATION

Corresponding Authors

Yinghui Sun – College of Chemical Engineering, Inner Mongolia University of Technology, Hohhot 010051, People's Republic of China; Inner Mongolia Key Laboratory of

Industrial Catalysis, Hohhot 010051, People's Republic of China; orcid.org/0000-0002-5302-188X; Phone: +86471 6575722; Email: syh9025@imut.edu.cn; Fax: +86471 6575722

Jie Bai – College of Chemical Engineering, Inner Mongolia University of Technology, Hohhot 010051, People's Republic of China; Inner Mongolia Key Laboratory of Industrial Catalysis, Hohhot 010051, People's Republic of China; orcid.org/0000-0002-7662-8238; Email: baijie@imut.edu.cn

Authors

Yu Su – College of Chemical Engineering, Inner Mongolia University of Technology, Hohhot 010051, People's Republic of China; Inner Mongolia Key Laboratory of Industrial Catalysis, Hohhot 010051, People's Republic of China

Ying Li – College of Chemical Engineering, Inner Mongolia University of Technology, Hohhot 010051, People's Republic of China; Inner Mongolia Key Laboratory of Industrial Catalysis, Hohhot 010051, People's Republic of China

Chunping Li – College of Chemical Engineering, Inner Mongolia University of Technology, Hohhot 010051, People's Republic of China; Inner Mongolia Key Laboratory of Industrial Catalysis, Hohhot 010051, People's Republic of China

Tong Xu – College of Chemical Engineering, Inner Mongolia University of Technology, Hohhot 010051, People's Republic of China; Inner Mongolia Key Laboratory of Industrial Catalysis, Hohhot 010051, People's Republic of China

Complete contact information is available at:
<https://pubs.acs.org/10.1021/acsomega.2c02400>

Notes

The authors declare no competing financial interest.

ACKNOWLEDGMENTS

We gratefully acknowledge the support from the National Natural Science Foundation of China (no. 21766022).

REFERENCES

- (1) Suzuki, A. Cross-Coupling Reactions of Organoboranes: An Easy Way to Construct C-C Bonds (Nobel Lecture). *Angew. Chem., Int. Ed.* **2011**, *50*, 6722–6737.
- (2) Choudary, B. M.; Madhi, S.; Chowdari, N. S.; Kantam, M. L.; Sreedhar, B. Layered Double Hydroxide Supported Nanopalladium Catalyst for Heck-, Suzuki-, Sonogashira-, and Stille-Type Coupling Reactions of Chloroarenes. *J. Am. Chem. Soc.* **2002**, *124*, 14127–14136.
- (3) Lei, M.; Tang, Y.; Wang, H.; Zhu, L.; Zhang, G.; Zhou, Y.; Tang, H. A catalytic strategy for rapid cleavage of C-Cl bond under mild conditions: Effects of active hydrogen induced by Pd nanoparticles on the complete dechlorination of chlorobenzenes. *Chem. Eng. J.* **2021**, *419*, 129510.
- (4) Dhawa, U.; Kaplaneris, N.; Ackermann, L. Green strategies for transition metal-catalyzed C-H activation in molecular syntheses. *Org. Chem. Front.* **2021**, *8*, 4886–4913.
- (5) Tao, X.; Long, R.; Wu, D.; Hu, Y.; Qiu, G.; Qi, Z.; Li, B.; Jiang, R.; Xiong, Y. Anchoring Positively Charged Pd Single Atoms in Ordered Porous Ceria to Boost Catalytic Activity and Stability in Suzuki Coupling Reactions. *Small* **2020**, *16*, No. e2001782.
- (6) Tang, H.; Wei, J.; Liu, F.; Qiao, B.; Pan, X.; Li, L.; Liu, J.; Wang, J.; Zhang, T. Strong Metal-Support Interactions between Gold Nanoparticles and Nonoxides. *J. Am. Chem. Soc.* **2016**, *138*, 56–59.
- (7) Zhang, A.; Liang, Y.; Zhang, H.; Geng, Z.; Zeng, J. Doping regulation in transition metal compounds for electrocatalysis. *Chem. Soc. Rev.* **2021**, *50*, 9817–9844.
- (8) Lu, L.; Zou, S.; Fang, B. The Critical Impacts of Ligands on Heterogeneous Nanocatalysis: A Review. *ACS Catal.* **2021**, *11*, 6020–6058.
- (9) Zhang, F.; Jin, J.; Zhong, X.; Li, S.; Niu, J.; Li, R.; Ma, J. Pd immobilized on amine-functionalized magnetite nanoparticles: a novel and highly active catalyst for hydrogenation and Heck reactions. *Green Chem.* **2011**, *13*, 1238.
- (10) Fang, Y.; Wang, E. Simple and direct synthesis of oxygenous carbon supported palladium nanoparticles with high catalytic activity. *Nanoscale* **2013**, *5*, 1843–1848.
- (11) Feng, G.; Liu, F.; Lin, C.; Li, W.; Wang, S.; Qi, C. Crystalline mesoporous γ -Al₂O₃ supported palladium: Novel and efficient catalyst for Suzuki-Miyaura reaction under controlled microwave heating. *Catal. Commun.* **2013**, *37*, 27–31.
- (12) Li, W.; Zhang, B.; Li, X.; Zhang, H.; Zhang, Q. Preparation and characterization of novel immobilized Fe₃O₄@SiO₂@mSiO₂-Pd(0) catalyst with large pore-size mesoporous for Suzuki coupling reaction. *Appl. Catal., A* **2013**, *459*, 65–72.
- (13) Wei, S.; Ma, Z.; Wang, P.; Dong, Z.; Ma, J. Anchoring of palladium (II) in functionalized SBA-16: An efficient heterogeneous catalyst for Suzuki coupling reaction. *J. Mol. Catal. A: Chem.* **2013**, *370*, 175–181.
- (14) Wang, P.; Liu, H.; Niu, J.; Li, R.; Ma, J. Entangled Pd complexes over Fe₃O₄@SiO₂ as supported catalysts for hydrogenation and Suzuki reactions. *Catal. Sci. Technol.* **2014**, *4*, 1333.
- (15) Bao, G.; Bai, J.; Li, C. Synergistic effect of the Pd-Ni bimetal/carbon nanofiber composite catalyst in Suzuki coupling reaction. *Org. Chem. Front.* **2019**, *6*, 352–361.
- (16) Deng, J.; Ren, P.; Deng, D.; Bao, X. Enhanced electron penetration through an ultrathin graphene layer for highly efficient catalysis of the hydrogen evolution reaction. *Angew. Chem., Int. Ed.* **2015**, *54*, 2100–2104.
- (17) Deng, D.; Yu, L.; Chen, X.; Wang, G.; Jin, L.; Pan, X.; Deng, J.; Sun, G.; Bao, X. Iron encapsulated within pod-like carbon nanotubes for oxygen reduction reaction. *Angew. Chem., Int. Ed.* **2013**, *52*, 371–375.
- (18) Biffis, A.; Centomo, P.; Del Zotto, A. D.; Zecca, M. Pd Metal Catalysts for Cross-Couplings and Related Reactions in the 21st Century: A Critical Review. *Chem. Rev.* **2018**, *118*, 2249–2295.
- (19) Ashworth, I. W.; Campbell, A. D.; Cherryman, J. H.; Clark, J.; Crampton, A.; Eden-Rump, E. G. B.; Evans, M.; Jones, M. F.; McKeever-Abbas, S.; Meadows, R. E.; Skilling, K.; Whittaker, D. T. E.; Woodward, R. L.; Inglesby, P. A. Process Development of a Suzuki Reaction Used in the Manufacture of Lanabecestat. *Org. Process Res. Dev.* **2018**, *22*, 1801–1808.
- (20) Pérez-Lorenzo, M. Palladium Nanoparticles as Efficient Catalysts for Suzuki Cross-Coupling Reactions. *J. Phys. Chem. Lett.* **2012**, *3*, 167–174.
- (21) Ling, S.; Qin, Z.; Huang, W.; Cao, S.; Kaplan, D. L.; Buehler, M. J. Design and function of biomimetic multilayer water purification membranes. *Sci. Adv.* **2017**, *3*, No. e1601939.
- (22) Yang, Q.; Su, Y.; Chi, C.; Cherian, C. T.; Huang, K.; Kravets, V. G.; Wang, F. C.; Zhang, J. C.; Pratt, A.; Grigorenko, A. N.; Guinea, F.; Geim, A. K.; Nair, R. R. Ultrathin graphene-based membrane with precise molecular sieving and ultrafast solvent permeation. *Nat. Mater.* **2017**, *16*, 1198–1202.
- (23) Li, S.; Huang, X.; Wan, Z.; Liu, J.; Lu, L.; Peng, K.; Schmidt-Ott, A.; Bhattarai, R. Green synthesis of ultrapure La(OH)₃ nanoparticles by one-step method through spark ablation and electrospinning and its application to phosphate removal. *Chem. Eng. J.* **2020**, *388*, 124373.
- (24) Yu, D.; Jie, J.; Wang, J.; Li, C. Design and fabrication of PdO/Ce_xO_y composite catalysts with coaxial nanotube and studies of their synergistic performance in Suzuki-Miyaura reactions. *J. Catal.* **2018**, *365*, 195–203.

(25) Akbar, K.; Jeon, J. H.; Kim, M.; Jeong, J.; Yi, Y.; Chun, S.-H. Bifunctional Electrodeposited 3D NiCoSe₂/Nickel Foam Electro-catalysts for Its Applications in Enhanced Oxygen Evolution Reaction and for Hydrazine Oxidation. *ACS Sustain. Chem. Eng.* **2018**, *6*, 7735–7742.

(26) Wang, X.; Zhang, X.; Pandharkar, R.; Lyu, J.; Ray, D.; Yang, Y.; Kato, S.; Liu, J.; Wasson, M. C.; Islamoglu, T.; Li, Z.; Hupp, J. T.; Cramer, C. J.; Gagliardi, L.; Farha, O. K. Insights into the Structure–Activity Relationships in Metal–Organic Framework-Supported Nickel Catalysts for Ethylene Hydrogenation. *ACS Catal.* **2020**, *10*, 8995–9005.

(27) Collins, G.; Schmidt, M.; O'Dwyer, C.; McGlacken, G.; Holmes, J. D. Enhanced Catalytic Activity of High-Index Faceted Palladium Nanoparticles in Suzuki–Miyaura Coupling Due to Efficient Leaching Mechanism. *ACS Catal.* **2014**, *4*, 3105–3111.

(28) Yang, Y.; Reber, A. C.; Gilliland, S. E.; Castano, C. E.; Gupton, B. F.; Khanna, S. N. More than just a support: Graphene as a solid-state ligand for palladium-catalyzed cross-coupling reactions. *J. Catal.* **2018**, *360*, 20–26.

(29) Zhao, H.; Li, L.; Wang, J.; Wang, R. Spherical core-shell magnetic particles constructed by main-chain palladium N-heterocyclic carbenes. *Nanoscale* **2015**, *7*, 3532–3538.

(30) Sheng, Z.-H.; Shao, L.; Chen, J.-J.; Bao, W.-J.; Wang, F.-B.; Xia, X.-H. Catalyst-Free Synthesis of Nitrogen-Doped Graphene via Thermal Annealing Graphite Oxide with Melamine and Its Excellent Electrocatalysis. *ACS Nano* **2011**, *5*, 4350–4358.

(31) Liu, B.; Yan, Z.; Xu, T.; Wang, J.; Li, C.; Gao, R.; Bai, J. Promoting electron transfer of surface oxygen vacancies in Pd/CeO₂-RE via doping engineering for enhancing catalytic activity in Suzuki coupling reaction. *J. Catal.* **2021**, *399*, 15–23.

(32) Thomas, A. A.; Denmark, S. E. Pre-transmetalation intermediates in the Suzuki–Miyaura reaction revealed: The missing link. *Science* **2016**, *352*, 329.

(33) Carrow, B. P.; Hartwig, J. F. Distinguishing between pathways for transmetalation in Suzuki–Miyaura reactions. *J. Am. Chem. Soc.* **2011**, *133*, 2116–2119.